ISSN: 2694-1708
DOI: 10.33552/ICBC.2026.03.000572
Insights in Chemistry and Biochemistry
Iris Publishers

Mini Review

Ammonia Decomposition for Hydrogen Production: From Catalyst Design to System Integration

Pei Xiong[1*], Changheng Huang[1], Ao Xu[1], Jike Wang[1*]

Institute for Advanced Studies, Wuhan University; Wuhan, 430000, China.

Corresponding authors: **Jike Wang**, *Institute for Advanced Studies, Wuhan University; Wuhan, 430000, China.*

Received Date: August 31, 2026

Published Date: September 25, 2026

Abstract

Ammonia has emerged as a promising liquid hydrogen carrier owing to its high hydrogen storage density (17.6 wt%), well-established infrastructure, and carbon-free nature. The core challenge in ammonia decomposition is to achieve efficient and stable hydrogen release under mild conditions. This mini review focuses on thermocatalytic ammonia decomposition and summarizes recent breakthroughs along two main directions: catalyst design and reactor–system integration. The mechanistic origin of catalytic activity is rationalized via the nitrogen chemisorption energy–activity volcano relationship. Notable advances include Ru-based catalysts with atomically dispersed active sites, non-noble metal alternatives (Fe, Co, Ni), vacancy engineering, and membrane reactor coupling. Finally, we emphasize that the transition from catalyst innovation to system-level optimization is essential for practical applications.

Keywords: Ammonia decomposition; Hydrogen production; Catalyst design; System integration.

Abbreviations: NH_3: Ammonia; H_2: Hydrogen; Ru: Ruthenium; Fe: Iron; Ni: Nickle; Co: Cobalt; CeO_2: Cerium dioxide; La_2O_3: Lanthanum oxide; Y_2O_3: Yttrium oxide; CNTs: Carbon nanotubes; MWCNTs: Multi-walled carbon nanotubes; SACs: Single-atom catalysts; PEDMADS: Plasma-enhanced dual membrane ammonia decomposition system; TEA: Techno-economic analysis; GWP: Global warming potential

Introduction

The large-scale application of hydrogen energy has long been constrained by storage and transportation bottlenecks. High-pressure gaseous hydrogen (H_2) storage (35 to 70 MPa) consumes substantial energy and poses safety hazards, while liquid hydrogen storage requires cooling to −253 °C, with energy consumption accounting for 25% to 35% of the hydrogen energy itself.[1] Ammonia (NH_3) precisely addresses these shortcomings. It can be liquefied at approximately 8 atm at room temperature, possesses a hydrogen mass fraction of 17.6 wt% and an energy density of 3.5 kWh/kg, and benefits from a mature global infrastructure for synthesis, storage, transportation, and distribution [2]. The NH_3 decomposition reaction ($2\ NH_3 \rightleftharpoons N_2 + 3\ H_2$, $\Delta H = +92$ kJ/mol) is thermodynamically favorable above 400 °C, but kinetically limited by the high activation energy (>100 kJ/mol) associated with N–H bond cleavage and N_2 desorption [3,4]. The microscopic mechanism, established by Ertl and co-workers on Fe single crystals, involves NH_3 adsorption, stepwise dehydrogenation ($NH_3 \rightarrow NH_2 \rightarrow NH \rightarrow N$), H_2 formation/desorption, and N_2 recombination/desorption. [5] A critical insight from DFT calculations is the volcano-shaped relationship between catalytic activity and nitrogen chemisorption energy ($Q_{N(0)}$): the active surface must bind nitrogen sufficiently strongly to facilitate N–H bond breaking, yet weakly enough to allow N_2 desorption and prevent poisoning [3,4]. This volcano relationship identifies Ru as the most active single metal [4]. Over

the past four years, approximately ~50 review articles have been indexed in Web of Science, reflecting the rapid evolution of this field [6, 7].

In this mini review, we focus on thermocatalytic NH_3 decomposition and summarize recent breakthroughs along two main directions: catalyst active site design and reactor–system integration. The catalyst design section covers Ru-based catalysts, non-noble metal alternatives (Fe, Ni, Co), single-atom catalysis, and vacancy engineering. The reactor integration section discusses membrane reactors, plasma-assisted processes, and microreactor technologies. We conclude with an outlook on future directions and the critical transition from catalyst innovation to system-level optimization. Figure 1 provides a schematic overview of the overall framework, visually summarizing the flow from catalyst design through reactor intensification to downstream.

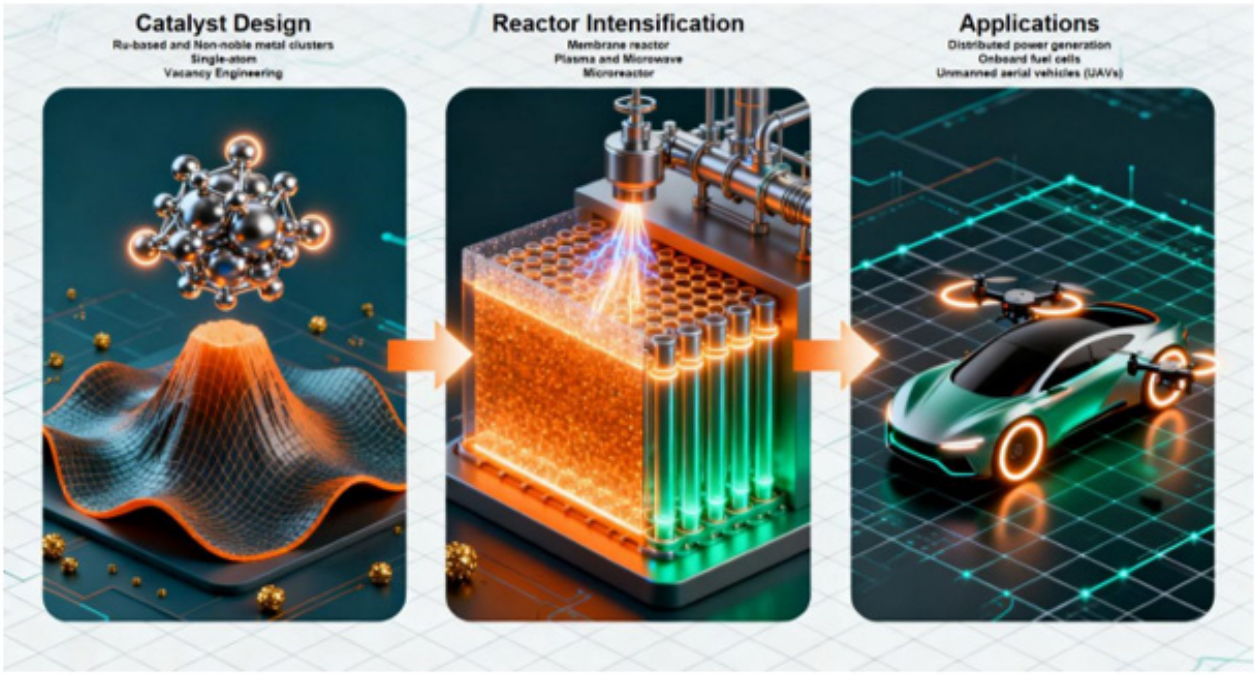

Figure 1: Schematic overview of NH_3 decomposition for H_2 production. The left and center panels illustrate the two key research frontiers discussed in this review: catalyst design and reactor intensification; the volcano curve rationalizes the activity trend of different metals based on nitrogen chemisorption energy. The right panel shows the downstream application scenarios enabled by these advances, including distributed power generation, onboard fuel cells, and unmanned aerial vehicles.

Breakthroughs in Catalyst Design: From Noble Metals to Non-Noble Metals, from Nanoparticles to Single Atoms

Catalyst design remains the cornerstone of low-temperature NH3 decomposition, where the trade-off between noble metal excellence and non-noble metal practicality defines the research frontier.

Ru-based catalysts remain the benchmark for low-temperature activity, with their optimal $Q_{N(0)}$ (~134 kcal mol^{-1}) [4]. $Ru/La_2Ti_2O_7$ achieves 66.5% NH_3 conversion at 450 °C with an extremely low Ru loading (~1.4 wt%), while $Ru/LaTiO_2N$ increases conversion to 76.1% with an H_2 production rate of 1,556 mmol g_{Ru}^{-1} min^{-1} and stable operation for 140 hours [8]. Beyond conventional supported Ru, recent advances exploit atomically dispersed Ru on polar MgO(111) surfaces, where close-packed Ru ensembles exhibit superior performance over stepped sites [9]. Additionally, confined Ru sites within 13X zeolite create frustrated Lewis pairs that facilitate dynamic hydrogen transfer, achieving ultrahigh H_2 production [10]. Despite its excellence, Ru's scarcity and high cost, coupled with its substantial global warming potential [11,12] drive the search for non-noble alternatives.

Fe-based catalysts, widely used in industrial Haber-Bosch synthesis, offer a cost advantage of approximately 50,000 times over Ru [13]. However, Fe suffers from strong Fe–N bond enthalpy, promoting surface nitride formation that poisons active sites; this deactivation can be reversed at higher temperatures, though often accompanied by irreversible sintering [4].

Ni-based catalysts are among the best-performing non-noble metals, with optimal activity observed at particle sizes of 1.8 to 2.9 nm on Al_2O_3.[14] Basic and defect-rich oxide supports (CeO_2, La_2O_3, $Gd\text{-}CeO_2$) enhance Ni dispersion and metal–support interactions. Rare earth promoters (Ce, La) improve both low-temperature and high-temperature stability, while bimetallic systems such as Ni-Co and Ni-Fe broaden the operating temperature window [15, 16].

Co-based catalysts have garnered significant attention due to their weaker nitrogen binding affinity than Fe and Ni, reflected in a 27 kJ mol-1 reduction in activation energy compared to Fe-based systems [17]. As summarized in Table 1, Co catalysts supported on MgO-La_2O_3 achieve 92% NH_3 conversion at 550°C [18]. while Co/MWCNTs reach 75% conversion at 500°C [19]. The superior performance of carbon supports is attributed to their mechanical stability, favorable metal–support interaction, and enhanced electron transfer that alleviates nitrogen desorption energy.[20] Alkali and alkaline earth promoters (K, Cs, Ba, La) further boost activity by increasing support basicity and facilitating electron donation to Co nanoparticles [18, 21, 22].

Table 1: Some Co-based catalysts for NH_3 decomposition (Pure NH_3 feed, atmospheric pressure).

Catalyst	Support	Promoter	T (°C)	NH_3 Conv. (%)	Ref.
Co	$MgOLa_2O_3$	La	550	92	[18]
Co	MWCNTs	–	500	75	[19]
Co	CNTs	–	500	61	[20]
Co	$LaCoO_x$/NC/SBA15	La	500	90	[22]

At the structural level, single-atom catalysts (SACs) show great potential. Co-Ba/Y_2O_3 with in situ constructed single-atom Ba promoter sites exhibits significantly enhanced activity [23]. Vacancy engineering lowers the energy barriers for N–H activation and N_2 desorption (50 to 60 kJ/mol), enabling catalysis at 200 to 500°C A period is needed here. The Ni-CeO_{2-x}/CNTs photothermal catalyst achieves 298.4 mmol g_{cat}^{-1} min^{-1} under full-spectrum illumination [25]. Recently, a Ru-free strained heterostructure catalyst enabled efficient low-temperature NH_3 cracking, achieving Ru-comparable performance [26]. Moreover, a Tammann-temperature-guided synthesis strategy for core@shell metal@metal-oxide catalysts offers a versatile route to thermally stable nanostructures [27].

Reactor and System Integration: Toward Low-Temperature Efficient Decomposition

Beyond catalyst development, reactor engineering and system integration are equally critical for overcoming the thermodynamic equilibrium limitations inherent to NH_3 decomposition. Even with high-performance catalysts, conventional fixed-bed reactors face thermodynamic equilibrium constraints at low temperatures, as the reversible nature of NH_3 decomposition restricts the maximum achievable conversion at a given temperature. Process intensification strategies, such as microwave heating, photothermal coupling, thermoelectric synergy, and plasma assistance, can reduce the required temperature by ~100 °C and enhance catalytic activity by 2 to 5 times, offering viable pathways to circumvent equilibrium limitations [28]. Membrane reactors represent one of the most effective approaches to shift the equilibrium toward complete conversion by in situ selective removal of H_2 from the reaction zone, following Le Chatelier's principle. By integrating H_2 separation with the reaction step, membrane reactors not only enhance NH_3 conversion at lower temperatures but also deliver high-purity H_2 directly, eliminating the need for downstream purification [28]. The plasma-enhanced dual-membrane NH_3 decomposition system (PEDMADS) exemplifies this concept: it integrates low-temperature plasma catalysis, a 1.8-μm-thick palladium membrane for H_2 separation (>87% recovery), and an S-1 zeolite membrane for unreacted NH_3 recovery [29]. At 400 °C, this system achieves an H_2 space-time yield of 1,567 mmol g^{-1} h^{-1}; plasma alone gives 52.1% conversion, and membrane removal further increases this by 24.8% to 65.0%. Techno-economic analysis shows a levelized cost of $0.92/kg H_2 and a 95.9% carbon footprint reduction compared to conventional thermal processes [29]. Beyond Pd-based membranes, microporous silica and zeolite membranes are also under active development, though their H_2/N2 selectivity and long-term stability remain challenging.

The synergy between different process intensification strategies often yields performance beyond the sum of their individual contributions. The integration of plasma with catalytic materials, for instance, exploits both the non-equilibrium chemistry of plasma and the selective activity of catalysts, driving the reaction at temperatures 200 to 300°C lower than conventional thermocatalysis [30]. This synergy arises from plasma-generated reactive species (e.g., NH_2, NH, N radicals) that bypass the high-barrier thermal pathways on catalyst surfaces. Microreactor technology also shows promise for distributed and on-demand H_2 production: a microcombustor–microreformer system with Ru achieves 98% conversion and 5.4 W H_2 output, while microchannel reactors reach 95% to 99% conversion with 75% catalyst saving [31]. The high surface-to-volume ratio and enhanced heat/mass transfer characteristics of microreactors enable precise temperature control, which is critical for this strongly endothermic reaction.

Beyond thermal and plasma-driven routes, alternative energy inputs have been explored to lower the energy barrier of NH_3 decomposition. Microwave-assisted decomposition leverages the selective heating of catalytic active sites, achieving significant energy savings and enhanced conversion at lower bulk temperatures [28]. Photothermal catalysis, as exemplified by the Ni-CeO_{2-x}/CNTs system, couples solar illumination with catalytic activity, achieving an H_2 production rate of 298.4 mmol g_{cat}^{-1} min^{-1} under full-spectrum light [25]. Electrocatalytic and photocatalytic NH_3 decomposition are still in their infancy but offer the potential for direct integration with renewable electricity or solar energy. Looking beyond conventional reactor architectures, a synergistic "nitrogen trap" and "hydrogen pump" strategy for spatially decoupled decomposition has been proposed, offering a new paradigm for enhancing conversion efficiency through reactor architecture innovation [32].

Application Prospects and Future Directions

The application scenarios of NH_3 decomposition for hydrogen production are expanding from centralized production to distributed power, onboard fuel cells, and unmanned aerial vehicles [31]. Techno-economic analysis shows a re-conversion cost of \$1.856/kg H_2 for Ru-based catalysts versus \$1.995/kg H_2 for Ni-based catalysts at 10 bar [33]. With renewable integration, NH_3 decomposition becomes cost-competitive.

Future directions include: (1) lowering non-noble metal catalyst operating temperature below 350°C, with recent Ni-based SACs showing promise near 300°C; (2) synergizing thermocatalysis, photocatalysis, electrocatalysis, and plasma catalysis; (3) machine learning-accelerated catalyst design, transitioning from trial-and-error to prediction; and (4) full-chain optimization integrating catalyst design, reactor engineering, thermal management, and purification. The NH_3 decomposition is moving from laboratory to industrial demonstration, and system-level integration will be the key breakthrough.

Acknowledgments

This work was financially supported by the Postdoctoral Fellowship Program of CPSF under Grant Number GZC20241255, the Postdoctoral General Fund of CPSF under Grant Number 2024M762475, the Hubei Province Postdoctoral Talent Introduction Project (2024HBBHJD078) and the Hubei Province Innovative Talent Training Program (2025HBBSHCXB096).

Competing interests

Authors declare that they have no competing interests.

References

1. JO Abe, API Popoola, E Ajenifuja, OM Popoola (2019) Hydrogen energy, economy and storage: Review and recommendation. Int J Hydrog Energy 44(29): 15072-15086.
2. A Valera-Medina, H Xiao, M Owen-Jones, WIF David, PJ Bowen (2018) Ammonia for power. Prog. Energy Combust. Sci 69: 63-102.
3. A Boisen, S Dahl, J Norskov, C Christensen (2005) Why the optimal ammonia synthesis catalyst is not the optimal ammonia decomposition catalyst J Catal 230(2): 309-312.
4. JC Ganley, FS Thomas, EG Seebauer RI Mase (2004) A priori catalytic activity correlations: the difficult case of hydrogen production from ammonia. Catal Lett 96: 117-122.
5. G Ertl, M Huber (1980) Mechanism and kinetics of ammonia decomposition on iron. J. Catal 61: 537-539.
6. DNHA Pg Haji Omar Ali, H Suhaimi, PE Abas (2026) From catalyst to system:a systematic review of simulation-based modelling of ammonia decomposition for hydrogen production. Hydrogen 7(1): 37.
7. MA Aslam, MS Abbas, RM Irfan, R Ahmad (2025) From ammonia to hydrogen: evolution of ruthenium-based catalysts. ACS Catal 15(21): 18631-18662.
8. XY Guo, JH Wang, TZ Li, K Xu, CJ Jia, et al. (2025) Multiple-atom-site catalysts for highly efficient hydrogen production from ammonia decomposition over Ru/LaxTiyA (A = O, N). J. Rare Earths).
9. H Fang, S Wu, T Ayvali, J Zheng J, Fellowes et al. (2023) Dispersed surface Ru ensembles on MgO(111) for catalytic ammonia decomposition. Nat Commun 14(1): 647.
10. KC Leung, S Hong, G Li, Y Xing, BKY Ng, et al. (2023) Confined Ru Sites in a 13X Zeolite for Ultrahigh H2 Production from NH3 Decomposition. J Am Chem Soc 145(26): 14548-14561.
11. P Nuss, MJ Eckelman (2014) Life cycle assessment of metals: a scientific synthesis. PLoS One 9(7): e101298.
12. I Lucentini, X Garcia, X Vendrell, J Llorca (2021) Review of the decomposition of ammonia to generate hydrogen. Ind Eng Chem Res 60(51): 18560-18611.
13. M Feyen, C Weidenthaler, R Guttel, K Schlichte, U Holle, et al. (2011) High-temperature stable, iron-based core-shell catalysts for ammonia decomposition. Chemistry 17(2): 598-605.
14. J Zhang, H Xu, W Li (2005) Kinetic study of NH3 decomposition over Ni nanoparticles: The role of La promoter, structure sensitivity and compensation effect. Appl. Catal. A: General 296(2): 257-267.
15. S Mukherjee, SV Devaguptapu, A Sviripa, CRF Lund, G Wu (2018) Low-temperature ammonia decomposition catalysts for hydrogen generation. Appl. Catal. B: Environ 226: 162-181.
16. H Yan, YJ Xu, YQ Gu, H Li, X Wang, et al. (2016) Promoted multimetal oxide catalysts for the generation of hydrogen via ammonia decomposition. J. Phys. Chem. C 120(14): 7685-7696.
17. Z Lendzion-Bieluń, R Pelka, W Arabczyk (2008) Study of the kinetics of ammonia synthesis and decomposition on iron and cobalt catalysts. Catal. Lett. 129(1-2): 119-123.
18. XY Guo, JH Wang, Q Zhang, TZ Li, H Dong, et al. (2024) Alkaline earth metal promoted hydrogen production from ammonia decomposition over Ni/La2O3-based catalysts. Appl. Catal. B: Environ. 348: 123844.
19. H Zhang, YA Alhamed, W Chu, Z Ye, A AlZahrani, et al. (2013) Controlling Co-support interaction in Co/MWCNTs catalysts and catalytic performance for hydrogen production via NH3 decomposition. Appl. Catal. A: General 464-465: 156-164.
20. H Zhang, YA Alhamed, A Al-Zahrani, M Daous, H Inokawa, et al. (2014) Tuning catalytic performances of cobalt catalysts for clean hydrogen generation via variation of the type of carbon support and catalyst post-treatment temperature. Int. J. Hydrog. Energy 39(31): 17573-17582.
21. D Varisli, NG Kaykac (2012) COx free hydrogen production over cobalt incorporated silicate structured mesoporous catalysts. Appl. Catal. B: Environ 127: 389-398.
22. X Han, M Hu, J Yu, X Xu, P Jing, et al. (2023) Dual confinement of LaCoOx modified Co nanoparticles for superior and stable ammonia decomposition. Appl. Catal. B: Environ. 328: 122534.
23. K Xu, YY Zhang, WW Wang, M Peng, JC Liu, et al. (2025) Single-atombarium promoter enormously enhanced non-noble metal catalyst for ammonia decomposition. Angew. Chem. Int. Ed. 64(4): e202416195.
24. A Salehabadi, J Zanganeh, B Moghtaderi (2026) Vacancy-engineered catalysis for enhanced hydrogen production from ammonia: A review. J. Alloys Compd. 1074: 189112.
25. R Tan, X Mu, X Wang, Y Kong, Q Ji, et al. (2025) Breakthrough photothermal ammonia decomposition via low-barrier Ni-CeO2-x interfaces on carbon nanotubes. Nat. Commun. 16(1): 11433.
26. P Xiong, J Li, Z Xu, Y Lin, RD Bennett, et al. (2025) Efficient low-temperature ammonia cracking enabled by strained heterostructure interfaces on Ru-free catalyst. Adv. Mater. 37(48): e2502034.
27. P Xiong, Z Xu, TS Wu, T Yang, Q Lei, et al. (2024) Synthesis of core@shell catalysts guided by Tammann temperature. Nat. Commun. 15(1): 420.
28. S Tang, Z Su, Y Wu, Y Liu, D Shi, et al. (2026) Advances in process intensification and reactor engineering for hydrogen production from ammonia decomposition. Int J Hydrog Energy 239: 155298.
29. S Meng, Y Chen, Z Cui, Y Gu, H Xiao, et al. (2025) Plasma-driven dual-membrane dystem for intensified hydrogen production with integrated ammonia recovery. J. Am. Chem. Soc. 147(46): 42949-42963.

30. Z Wang, H He, S Tan, T Xie, W Li, et al. (2025) Low-temperature plasma-assisted ammonia decomposition catalyzed with bimetallic catalysts: Kinetic study and energy-efficiency analysis. Int J Hydrog Energy 139: 730-739.

31. V Madadi Avargani, SA Amirsadat, SM Amirsadat (2026) Microchannel reactors for sustainable hydrogen production: From fundamentals to industrial scale-up. Renew. Sustain. Energy Rev. 238: 117052.

32. P Xiong, JZhang, C. Huang, MMJ Li, Z Xu, et al. (2026) Synergistic "nitrogen trap" and "hydrogen pump" strategy for spatially decoupled ammonia decomposition. ACS Catal.

33. M Chopra, N Srivastava, P Arora (2026) Decentralized hydrogen production via ammonia decomposition: process simulation, techno-economic, and environmental assessment. Fuel 415: 138463.